

## Monte Carlo simulation of the mixed alkali effect with cooperative jumps

Junko Habasaki

*Tokyo Institute of Technology, Nagatsuta 4259, Yokohama 226-8502, Japan*

Yasuaki Hiwatari

*Kanazawa University, Kakuma-machi Kanazawa 920-1192, Japan*

(Received 26 June 2000)

In our previous works on molecular dynamics (MD) simulations of lithium metasilicate ( $\text{Li}_2\text{SiO}_3$ ), it has been shown that the long time behavior of the lithium ions in  $\text{Li}_2\text{SiO}_3$  has been characterized by the component showing the enhanced diffusion (Lévy flight) due to cooperative jumps. It has also been confirmed that the contribution of such component decreases by interception of the paths in the mixed alkali silicate ( $\text{LiKSIO}_3$ ). Namely, cooperative jumps of like ions are much decreased in number owing to the interception of the path for unlike alkali-metal ions. In the present work, we have performed a Monte Carlo simulation using a cubic lattice in order to establish the role of the cooperative jumps in the transport properties in a mixed alkali glass. Fixed particles (blockage) were introduced instead of the interception of the jump paths for unlike alkali-metal ions. Two types of cooperative motions (a pull type and a push type) were taken into account. Low-dimensionality of the jump path caused by blockage resulted in a decrease of a diffusion coefficient of the particles. The effect of blockage is enhanced when the cooperative motions were introduced.

PACS number(s): 02.60.-x, 66.10.Ed, 66.30.-h

### I. INTRODUCTION

In alkali silicate glasses, transport coefficients, such as self-diffusion coefficients, markedly fall when a single alkali-metal ion is mixed with other alkali-metal ions; this phenomenon is referred to as the ‘‘mixed alkali effect’’ [1–3]. In our previous work, a large decrease of mean squared displacements by such mixing of alkali metal ions has been reproduced [4] in the simulation of  $\text{LiKSIO}_3$  glass, where the interception of the jump path among the unlike alkali-metal ion sites has been shown to occur at least in several hundreds ps region at 700 K. Examination of the potential energy surface reveals that a smaller alkali-metal ion becomes unstable if it enters the site previously occupied by a larger alkali-metal ion and vice versa [4–6]. The jump paths and motions of alkali-metal ions has been characterized by an analysis of fractal dimension. In simulations (up to the 1 ns region) for  $\text{Li}_2\text{SiO}_3$ , we have confirmed that the dynamics of Li ions have divided into slow and fast dynamics. Fast dynamics of the lithium ion has been characterized as Lévy flight [7,8], since the power law distribution of displacement of particles has been observed (distribution of characteristic scale for the jump motions). Cooperative jump motion is the main mechanism to determine the long time dynamics of the pure alkali silicate system [8,9]. On the other hand, single jumps cannot contribute to the long time diffusive motion because of large back-correlation probability due to local low-dimensional structure of the jump paths. A change in cooperative motion by mixing is suggested as an origin of the extraordinary large mixed alkali effect (4~5 orders of magnitude) [6,10]. However, quantitative assessment of the effect is still insufficient. Therefore, it is important to learn much detail about the role of the cooperative jumps in the mixed alkali effect. Determination of absolute value of the diffusion coefficients from molecular dynamics (MD) data is quite difficult because it requires a long simu-

lation time due to the time dependent character of the mean squared displacement and discontinuity of jump motions [8,11–13], and interconversion of fast dynamics and slow dynamics also cause large fluctuations of the mean squared displacement in the glassy state [14]. In the present work, Monte Carlo (MC) simulation has been used to examine how interception of the jump path affects the cooperative jump motions in some simplified cases.

### II. METHOD: MC SIMULATION

MC simulations were performed at 300 K using a cubic lattice of  $10 \times 10 \times 10$  with a periodic boundary condition. Lennard-Jones particles (argonlike) were used instead of alkali-metal ions. A distance between neighboring sites is set to be 3.9 Å. In each elementary step of the simulation, a particle 1 was chosen randomly and a direction was also chosen randomly, to which the ion attempts to jump. In the simulation without cooperative jumps, the jump was rejected if the neighboring site was occupied by another particle (or by the fixed particles mentioned later). If the neighboring site was vacant, the jump probability was determined by the Metropolis method. In the simulation with the cooperative jumps of pull type, the trial was rejected if the second site in the forward direction of particle 1 was occupied. When the second neighboring site was vacant, the second neighboring site in the opposite side was checked. If the site was occupied by another mobile particle 2, both 1 and 2 particles can try to move simultaneously. For the cooperative jumps of push type, the first neighboring site of particle 1 in the forward direction was checked. If the site was occupied by another mobile particle 2', the second neighboring site in the same direction was checked. When the site was occupied by fixed or mobile particle, the trial was rejected. If the first neighboring site was occupied by mobile particle 2' and the second neighboring site was vacant, both 1 and 2' particles

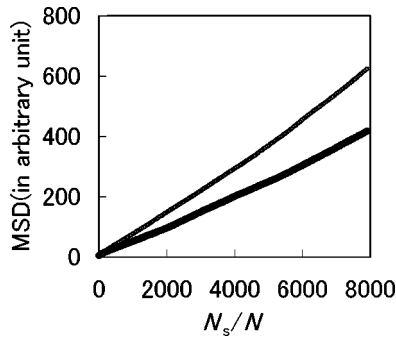


FIG. 1. MSD for the cases  $\circ$  (Pull+S) ( $N=700$ ,  $N_B=250$ ) and  $\bullet$  (S) ( $N=250$ ,  $N_B=0$ ).

could try to move simultaneously. (In the present simulation, pull type motion occurs taking precedence over the single jumps. This rule was introduced only for simplicity of the simulation and is not necessarily realistic. The ratio of single jumps to cooperative jumps should depend on the activation energy of these jumps. However, in the present MC simulations, we neglect the distribution of activation energies.)

The probability of the success of the cooperative jump was also determined by the Metropolis method. That is, it depends on the total potential energy of the system at the next step. A decrease in fractal dimension of the path was introduced by fixed particles. In some cases, the positions of selected particles were fixed during simulation time. After each trial, the time  $t$  was incremented by  $t_0/N$ , where  $N$  is the number of the mobile ions. The elementary step was repeated again and again until thermal equilibrium was reached. The acceptance ratio of the Metropolis method,  $A_c$ , the number's ratio of the successful jumps to jump trials,  $P_s$ , were calculated. The trials were continued in order to calculate the mean squared displacement until the number of the successful jumps ( $N_s$ ) becomes  $10\,000N$ . Although the value  $P_s$  becomes smaller when the number of total particles becomes larger, the error range of the  $D$  value was kept almost the same by this procedure. Five cases were examined and compared with each other:

- (i) Only single jumps were allowed (S).
- (ii) Pull type of cooperative motion was allowed in addition to single jumps (Pull+S).
- (iii) Push type of cooperative motion was allowed in addition to single jumps (Push+S).
- (iv) Both pull and push type of cooperative motions were allowed. Single jumps were not allowed (Pull+Push).
- (v) Both pull and push type cooperative motions were allowed in addition to single jumps (Pull+Push+S).

In Fig. 1, mean squared displacements (MSDs) of two cases were shown as examples. In the present work, apparent diffusion coefficients,  $D$ , were calculated from the slopes in the  $N_s=6000\sim 8000N$  region of MSD and  $P_s$  values. The MSDs tend to show a time dependent character in some cases. Such characters (especially for cases with cooperative motion) will be discussed in the future. The values were normalized by using  $D_0$  (for single jumps of  $N=250$  particles without blockage), since the back correlation probability in this case is almost  $1/6$  and is quite similar to the case for the free particle motion. That is,  $D_0 \sim \lim_{c \rightarrow 0} D(c)$ .

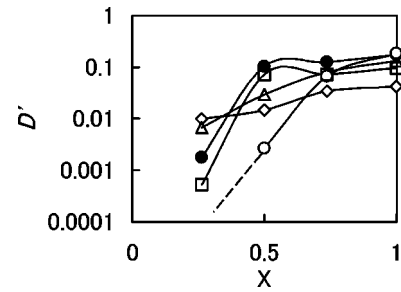


FIG. 2.  $D'$  values for the mobile particles are plotted against  $X=N/(N+N_B)$  for the case  $N+N_B=950$ , where the mobile particle and block particle play roles of two kinds of alkali-metal ions in the mixed alkali effect. Types of jumps allowed are  $\diamond$  (S),  $\square$  (Pull+S),  $\triangle$  (Push+S),  $\circ$  (Pull+Push), and  $\bullet$  (Pull+Push+S).

Our previous molecular dynamics (MD) studies based on the visualization and the fractal dimension analysis of the path in the mixed alkali-metal (LiKSIO<sub>3</sub>) glass revealed the following features [8–10]:

1. Each kind of alkali-metal ion clearly shows an independent path at least in the time scale of several tens to hundreds ps, which indicates the interception of the mutual jump paths.
2. Contribution of the cooperative jumps to the squared displacements decreases by mixing. The bulk velocity auto-correlation function is affected by mixing more significantly than the tracer function is.
3. Back-correlation of the jump motion becomes larger in the mixed alkali system. That is, each particle has local mobility.

Thus, the large decrease in dynamics in the mixed alkali-metal system is mainly caused by the mutual interception of the jump paths of unlike ions. This resulted in the decrease in forward-correlated jumps with the cooperative jump motion, which is the main mechanism of the conduction and/or diffusion in pure systems. In the mixed alkali system, the component showing accelerated diffusion was confirmed to be nearly absent in the MD simulation up to 1 ns at 700 K [11].

This result is quite different from that in the “dynamic structure model” [15,16], which has been proposed to explain the “mixed alkali effect,” where the unlike ion can enter the pathway and dynamically interfere the jump of the respective ions. Therefore, we neglected the change of the pathway during the simulation time in the present work, although such motion is observed in a longer time scale [12].

### III. RESULTS AND DISCUSSION

#### A. Diffusion Coefficients for fixed density ( $N+N_B=950$ ) cases

In Fig. 2,  $D'$  values for the systems containing  $N+N_B=950$  particles are shown, where  $X=N/(N+N_B)$ . The fixed particle play a role for the blockage by unlike alkali-metal ions in the mixed alkali case.  $D'$  (where  $D'=D/D_0X$ ) was used rather than  $D$  itself in this section. The factor  $X$  can be considered as a correction of time required for activation of jump motion, since in a real mixed alkali glass, unlike alkali ions also move in the independent paths. The order of  $D'$  at  $X=1$  ( $N+N_B=950$ ) was as follows. Note that the vertical axis is in log scale:

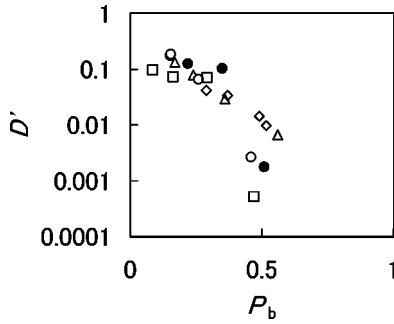


FIG. 3.  $D'$  values for the mobile particles are plotted against back correlation probability ( $P_b$ ) of the particles. Types of jumps allowed are the same as in Fig. 2

$$D'(Pull+Push+S) \sim D'(Pull+Push) > D'(Push+S) \\ > D'(Pull+S) > D'(S). \quad (1)$$

The order clearly means that the diffusion is accelerated by the existence of cooperative motions. Significant decreases of  $D'$  values were observed by mixing with block particles in every case. The blockage effect was enhanced considerably when cooperative motions were allowed in spite of the fact that only two particle motions were being taken into account. Thus, the rapid fall in conductivity seen in the dilute foreign alkali-metal region [3] of the mixed alkali system can be explained by the existence of the cooperative jumps. Namely, a blockage of the path at one site can affect many ions since the cooperative motions were intercepted. This explanation is in contrast to that in the ‘‘dynamic structure model,’’ where a large limiting slope was explained by the assumption that an unlike ion can enter the pathway and dynamically interfere with the jump of the respective ions.

The behavior of (Pull+S) slightly differed from that of (Push+S), although the probability of cooperative jumps of pull and push types should be the same. The difference is due to the fact that the pull type motion is allowed when the single type motion is also possible. On the other hand, single jump is impossible when the push type motion is allowed. Namely, the particle intercepted by other particle cannot jump without push type motion.

The rapid change of  $D'$  in the case (Pull+Push) began at lower concentration of blockage compared with the other cases. In this case,  $D'$  values are sensitive to the concentration of block particles.

In Fig. 3,  $D'$  values were plotted against back correlation probabilities ( $P_b$ ). As shown in Fig. 3,  $D'$  values decreased with increasing  $P_b$ . Namely,  $D'$  is a function of the geometrical correlation factor,  $f(c)$ . In general,  $D(c) = D_0(1 - c)f(c)$  and  $f(c)$  is directly related with  $P_b$ . The small deviation from this relation is due to the changes in an acceptance ratio ( $A_c$ ) of the Metropolis method, which depends on the character of the potential functions. The ratios for the  $N+N_B=950$  cases were found to be between 0.86  $\sim$  0.91. In high  $P_b$  regions,  $D'$  values were fairly smaller than the expected values, when both types of cooperative motions were considered. In these cases, the systems are near the percolation threshold, since some particles were trapped within a unit cell even after  $N_s = 10\,000N$  runs. Namely, a

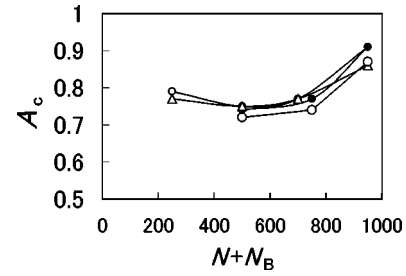


FIG. 4. Acceptance ratio of the Metropolis method,  $A_c$  is plotted against  $N+N_B$ . The types of jumps are  $\circ$  (S) without block;  $\bullet$  (S) with block ( $N_B=250$ );  $\triangle$  (Push+S) without block;  $\square$  (Push+S) with block ( $N_B=250$ ).

percolation threshold tends to shift toward to right in Fig. 2, if cooperative motions exist. This can be explained by the geometrical condition of the jump path, since the crooked path may allow only single jumps. A cooperative jump is effective to increase the  $D'$  values, while the jumps are sensitive to blockage. In the MD simulation of  $\text{Li}_2\text{SiO}_3$ , a memory of jump direction of Li ions is held and is one of the characteristics of Lévy flight dynamics [8]. In each elementary step of the present MC simulations, a direction of a particle 1, to which the particle attempts to jump was chosen randomly. Therefore, the correlation of the jump directions of successive jumps in MC simulations were caused only by the geometrical condition of particle positions.

#### B. Diffusion coefficients in the cases (S) and (Push+S) with and without block particles ( $N_B=250$ )

As a typical example of simple cooperative system,  $D$  values of case (Push+S) were compared with those of case (S) in this section.

In Fig. 4,  $A_c$  values are plotted against  $N+N_B$ . In the present MC simulations, the interaction with the block particle is the same as that with mobile particles. Therefore, the  $A_c$  value is a function of total number of particles. The result is consistent with those in the preceding section, where the acceptant ratio is almost constant for the case of fixed density ( $N+N_B=950$ ). As shown in Fig. 4,  $A_c$  values have the minima at the  $N+N_B=500$  region and the values for the case (S) is slightly larger than the case (Push+S). Observed  $D$  values were modified by the  $A_c$  values. Except for this,  $D$  values are determined mainly by geometrical correlation factors, as already been discussed.

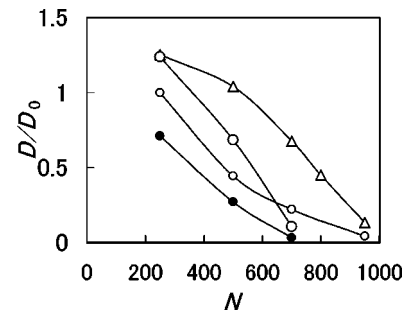


FIG. 5.  $D/D_0$  values are plotted against  $N$ .  $\circ$ , (S) without block;  $\bullet$ , (S) with block ( $N_B=250$ );  $\triangle$ , (Push+S) without block;  $\square$ , (Push+S) with block ( $N_B=250$ ).

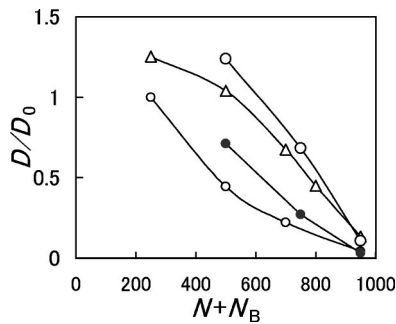


FIG. 6.  $D/D_0$  values are plotted against  $N+N_B$ . Symbols are the same as in Fig. 5.

In Figs. 5 and 6,  $D$  values were plotted against  $N$  and  $N+N_B$ , respectively. As clearly shown in the figures, the effect of block particles ( $N_B=250$ ) was larger in the case (Push+S) than in the case (S). In the lowest concentration, the motion of (Push+S) was not so much disturbed by the blockage.  $D/D_0$  values converged to 0 in every case at  $N+N_B=1000$  as expected, where all sites were occupied. This means that a mobility of a particle is suppressed by not only block particles but also by other mobile particles.  $D$  values for the cases with fixed block particles are larger than that without fixed block particles in the case of the same  $N+N_B$  values. This means that the addition of the fixed block particles decrease  $D$  but such effect is smaller than that of mobile particles.

In Fig. 7, the  $D/D_0$  values are multiplied by the number of mobile particles ( $N$ ). The value for the single jumps tends to decrease with increasing density. On the other hand, the curve for the case (Push+S) shows maximum at about  $N+N_B=500$ . This result can be explained as follows. With increasing density, the cooperative motion becomes dominant and is effective to cause high conductivity. However, due to high sensitivity of the cooperative motion to the den-

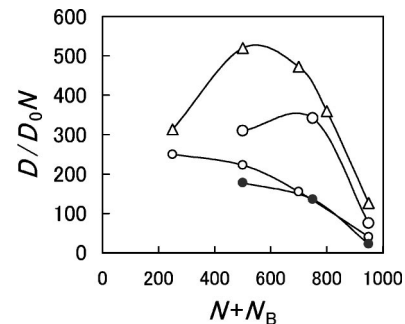


FIG. 7.  $D/D_0$  values are multiplied by the number of mobile particles ( $N$ ). Symbols are the same as in Fig. 5.

sity, the conductivity rapidly falls at higher density region. Thus, the existence of the maximum gives us a guiding principle to obtain high conductivity materials.

#### IV. CONCLUSION

In single jumps,  $D$  values decrease moderately by the blockages. On the other hand, with cooperative motion, blockage effect was larger especially in larger  $N$  region. That is, in dense materials, the cooperative jumps increase the  $D$  value, and the blockage effect becomes remarkable in such region. Some characteristics of Lévy flight, such as power law distribution of numbers of cooperative particles, were neglected here. However, effects of simple two particle motions are large enough to explain the large mixed alkali effect caused by the interception of the jump paths.

#### ACKNOWLEDGMENTS

Part of the calculations in this work were performed with the NEC SX3/34R computer at the Institute for Molecular Science at Okazaki. The CPU time is gratefully acknowledged for its availability.

- 
- [1] J. O. Isard, *J. Non-Cryst. Solids* **1**, 235 (1969).
  - [2] D. E. Day, *J. Non-Cryst. Solids* **21**, 343 (1976).
  - [3] M. D. Ingram, *Phys. Chem. Glasses* **28**, 215 (1987).
  - [4] J. Habasaki, I. Okada, and Y. Hiwatari, *J. Non-Cryst. Solids* **183**, 12 (1995).
  - [5] S. Balasubramanian and K. J. Rao, *J. Phys. Chem.* **97**, 8835 (1993); *J. Non-Cryst. Solids* **181**, 157 (1995).
  - [6] J. Habasaki, I. Okada, and Y. Hiwatari, *J. Non-Cryst. Solids* **208**, 181 (1996).
  - [7] M. F. Shlesinger, G. M. Zaslavsky, and J. Klafter, *Nature (London)* **363**, 31 (1993); J. Klafter, M. F. Shlesinger, and G. Zumofen, *Phys. Today* **49**, 33 (1996).
  - [8] J. Habasaki, I. Okada, and Y. Hiwatari, *Phys. Rev. B* **55**, 6309 (1997).
  - [9] J. Habasaki, I. Okada, and Y. Hiwatari, *Proceedings of the Fall Meeting, Material Research Society, Boston, 1996* [*Mater. Res. Soc. Symp. Proc.* **455**, 91 (1997)].
  - [10] J. Habasaki, I. Okada, and Y. Hiwatari, *Prog. Theor. Phys. Suppl.* **126**, 399 (1997).
  - [11] J. Habasaki, I. Okada, and Y. Hiwatari, *J. Phys. Soc. Jpn.* **67**, 2012 (1998).
  - [12] J. Habasaki and Y. Hiwatari, *Phys. Rev. E* **58**, 5111 (1998).
  - [13] J. Habasaki, I. Okada, and Y. Hiwatari, *Phys. Rev. E* **52**, 2681 (1995).
  - [14] J. Habasaki and Y. Hiwatari (unpublished).
  - [15] A. Bunde, M. D. Ingram, and P. Maass, *J. Non-Cryst. Solids* **172-174**, 1222 (1994).
  - [16] M. D. Ingram, *Glastech. Ber. Glass Sci. Technol.* **67**, 151 (1994).